ELSEVIER

Biochimica et Biophysica Acta 1190 (1994) 25–39

BBA Biochimica et Biophysica Acta

Polymorphic phase behavior of perfluoroalkylated phosphatidylcholines

Catherine Santaella [a], Pierre Vierling [a,*], Jean G. Riess [a], Tadeusz Gulik-Krzywicki [b], Annette Gulik [b], Bernard Monasse [c]

[a] *Laboratoire de Chimie Moléculaire, URA 426 au CNRS, Faculté des Sciences, Université de Nice-Sophia Antipolis, 06108 Nice Cédex 2, France*

[b] *Centre de Génétique Moléculaire, CNRS, 91190 Gif sur Yvette, France*

[c] *Ecole Supérieure des Mines de Paris, Sophia Antipolis, 06560 Valbonne, France*

(Received 30 June 1993)

Abstract

The polymorphic phase behavior of the *F*-alkyl modified phosphatidylcholines F*n*C*m*PC with F*n* = C_nF_{2n+1} and C*m* = $-(CH_2)_m-$ and the physicochemical properties of their aqueous dispersions have been investigated. We show that the supramolecular assemblies formed by F4C4PC, F6C4PC, F8C4PC and F4C10PC dispersed in water consist of liposomes. F6C10PC forms, as does F8C10PC, a ribbon-like phase (two-dimensional centered rectangular lattice) at 25°C, but on heating, it forms a lamellar phase. Upon cooling, the lamellar gel phase is metastable and converts slowly back into the ribbon-like phase. Analyses of the dispersions before and after heat sterilization and upon storage at 25°C reveal an exceptional stability of the F*n*C*m*PC-based liposomes which contrasts strongly with that of DPPC vesicles. This enhanced stability most likely arises from the increased hydrophobic character resulting from the presence of the perfluoroalkyl tails. The gel to fluid phase transition temperature of the F*n*C*m*PCs is found to be related to the total length of the hydrophobic chain and more markedly to the length of the perfluoroalkyl tail. This phase transition is first induced by the melting of the fluorocarbon chain. Each portion of the F*n* tail and of the hydrocarbon spacer experiences intrinsic changes of molecular motion with temperature. The partitioning of a lipophilic/hydrophilic paramagnetic probe between the aqueous and lipidic phases present in the F*n*C*m*PC dispersions shows that an increase in fluorophilic character results in a lower solubility of the probe in the membrane, thus reflecting a dramatic decrease of the membrane's lipophilicity.

Key words: Perfluoroalkylated phosphatidylcholine; Phospholipid; Liposome; Fluorinated liposome; Vesicle; Membrane; Polymorphism

1. Introduction

Vesicles formed from phospholipids (liposomes) provide chemical models for the study of biological membrane functions [1] as well as challenging drug carriers and delivery systems [2]. Vesicles made from pure monodispersed phospholipids have low stability. The development of more stable membranes usually requires multicomponent systems and elaborate formulations. Phospholipids, when used as emulsifiers, have also allowed the development of concentrated fluorocarbon emulsions destined to serve as artificial oxygen carrier and delivery systems [3]. The interest for such systems has grown as the scope of their potential applications has widened from temporary blood substitutes to numerous other therapeutic indications [4–6]. Although natural phospholipids are well accepted and routinely used in injectable preparations, they have their limitations and leave little leeway for varying the vesicles' and emulsions' characteristics and properties (particle size and size distribution, shelf stability, in-vivo recognition, uptake and acceptance, intravascular persistence, biodistribution...) [7]. Future progress in the above areas will aim at obviating these limitations and therefore at developing new lines of biocompatible membrane- and vesicle-forming amphiphiles. More generally one should underscore the lack of such strongly amphiphilic though biocompatible compounds.

* Corresponding author. Fax: +33 93529020.

SSDI 0005-2736(93)E0305-T

Accordingly, we have synthesized a series of analogs of phosphatidylcholines – the main components of natural phospholipids – in which each of the natural fatty acid chains is replaced by a saturated hydrocarbon spacer (C*m*) terminated by a perfluoroalkyl tail (F*n*) and linked to the glycerophosphocholine polar head through an ester junction (Fig. 1) [8a]. The perfluoroalkyl tails were expected (i) to increase the hydrophobicity of the membrane lipids, which usually leads to improved stability of the vesicle shell and (ii) to decrease the lipophilicity of the membranes they would form (fluorocarbons possess a very low affinity for both aqueous phases and hydrocarbons). Owing to their enhanced lipophobic and amphiphilic characters as compared to natural phosphatidylcholines, these *F*-modified phospholipids were expected to generate new polymorphic phase behaviors, diverse possibilities in forming bilayer or non-bilayer structures of original properties and, more particularly, to modify the interactions of these structures with biological compounds (proteins, enzymes...). They were also intended to combine, in a strongly amphiphilic structure, fluorophilicity (in which the most commonly used fluorocarbon emulsifiers, i.e., Pluronic F-68 and egg yolk phospholipids EYP, are missing), efficient emulsifying properties and biological compatibility. Indeed, the new *F*-alkylated glycerophosphocholines (i) form vesicles of exceptional shelf stability (as already reported in a preliminary communication, only minor changes in terms of particle size and size distribution are observed after ten months of storage at room temperature) [9], (ii) are very efficient emulsifiers or co-emulsifiers of fluorocarbons when used with EYP [9,10] and (iii) preliminary biocompatibility data indicate that they are well tolerated (i.v. LD_{50} in mice higher than 8 g/kg body weight), in spite of increased surface activity [8b].

Natural phospholipids, when dispersed in an aqueous phase, assemble into supramolecular structures, such as lipid bilayer and uni- or multilamellar vesicles. The interplay of four types of interactions (van der Waals attraction, hydrogen bonding, electrostatic and hydrophobic interactions) is responsible for the organization adopted by the lipids. In all cases, the properties of these arrangements depend upon the 'packing', which in turn depends on the molecular structure of the lipids [11,12]. It is now well-established that the length and degree of unsaturation of the hydrocarbon chains and the nature of the polar head (head-group type, hydration, degree of (de)protonation or ionization (charge), space filling characteristics) are crucial parameters, among others, in determining the phase behavior of phospholipids.

The structural variations permitted at the molecular level for the new fluorine-modified phosphatidylcholines (variable F*n* and C*m* lengths, hence variable F*n*/C*m* weights) allow stepwise adjustment of their physicochemical parameters (fluorophilicity/lipophilicity/ hydrophilicity balance) and properties (packing behavior, surface curvature, stability, crystal to liquid-crystal phase transition temperature, fluidity/rigidity, dynamics, permeability...) of the supramolecular structures they form. The similarity in size of hydrogen and fluorine atoms in organic compounds [13] instigated studies of fluorinated phospholipids where fluorine was to serve as a probe for membrane investigations [14]. It was found, however, that the substitution of one CH_2 group by a CF_2 group in each of the fatty acid chains of myristoyl phosphatidylcholine already caused significant perturbations in the bilayer structure [15]. It is also noteworthy that such fluorine-labeled phospholipids formed vesicles but led to non-ideal mixtures with the parent hydrocarbon phospholipids [16].

We report here the results of a detailed investigation of the polymorphic phase behavior and physicochemical properties of aqueous dispersions of the *F*-alkyl modified phosphatidylcholines F*n*C*m*PC. This paper is devoted to the morphological characterization, by freeze-fracture electron microscopy (FFEM), of the supramolecular assemblies formed by these F*n*C*m*PCs. The effect on vesicle size (obtained by light scattering spectroscopy measurements, LSS) and packing induced by the modification of the lipid chain is discussed. FFEM was also used to investigate dispersions obtained from the F*n*C*m*PCs starting either from thin-layered or from powdered lipids, as well as the impact of heat-sterilization on these dispersions. These are key issues when the in vivo use of such amphiphiles is contemplated. Their thermally-triggered phase behavior was studied by differential scanning calorimetry (DSC). X-ray diffraction and spectroscopic methods (^{19}F- and ^{31}P-NMR, EPR) were used to obtain structural and/or dynamical information. The impact of the molecular structure of the F*n*C*m*PCs on the physicochemical properties (lyotropism, thermotropism, lipophilicity) of the supramolecular systems they form in water is discussed. In all cases, the experimental data obtained are compared with those obtained for their hydrogenated phosphatidylcholine analogs.

2. Materials and methods

The synthesis and characterization (elemental analysis, ^{1}H-, ^{13}C-, ^{31}P-, ^{19}F-NMR spectra and IR spectroscopy) of the racemic F*n*C*m*PCs (Fig. 1) used in this study are described in Ref. 8a. Their purity was periodically controlled by TLC and/or HPLC. Dispersions of the lipids were prepared with a Branson B-30 sonifier. Particle sizes and size distributions were determined by light scattering spectroscopy (LSS) on a Coulter Model N4SD Sub-Micron Particle Analyser.

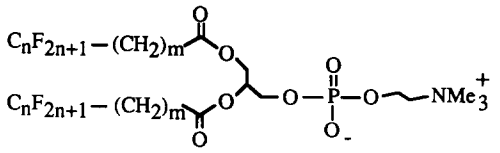

n = 4 , m = 4 : F4C4PC n = 4 , m = 10 : F4C10PC
n = 6 , m = 4 : F6C4PC n = 6 , m = 10 : F6C10PC
n = 8 , m = 4 : F8C4PC n = 8 , m = 10 : F8C10PC

Fig. 1. Structure of the *F*-alkyl-phosphatidylcholines and definition of their F*n*C*m*PC code name.

2.1. Preparation of the dispersions

Hepes (*N*-2-hydroxyethyl-1-piperazine-*N*'-2-ethanesulphonic acid), 10^{-2} M, pH 7 was used as a buffer for freeze-fracture experiments. Concentrations of phospholipids were 10–20 mmol/ml (2–3% w/v), except for compound F8C10PC whose concentration was 3.5 mmol/ml (0.5% w/v), in order to obtain stable dispersions. The lipids were dissolved in chloroform (for compounds F4C4PC and F4C10PC) or in a chloroform/methanol mixture (1 : 1, v/v) (compounds F6C4PC, F8C4PC, F6C10PC, F8C10PC). The solvents were then evaporated by rotation under argon to produce a uniform film. Residual traces of solvent were removed by storage under vacuum (10^{-3} mmHg, 2 h). The thin layers were hydrated with a Hepes buffer for 10 min above the phase transition temperature of the lipids (75–80°C), shaken for 1 min on a vortex mixer to produce a raw dispersion, then briefly sonicated (2–5 min, 3 mm titanium probe, dial 4–7, pulse 50). Dispersions were obtained from the powdered lipids using the same procedure but without the thin layer lipid step preparation. In the case of F6C10PC additional dispersions were also prepared from the powdered lipid by submitting the above dispersions to repeated heating-cooling cycles through the T_c of F6C10PC and further sonication. The samples (5 ml) were sterilized by autoclaving the dispersions for 15 min at 121°C under a pressure of 15 lb/in^2.

2.2. Freeze-fracture electron microscopy

The dispersions were prepared as described above. To prevent freeze damage, the samples were diluted with an equivalent volume of an aqueous solution of glycerol (50% w/w) and incubated at room temperature for 4 h before cryofixation. A small drop of each suspension (about 0.5 μl) was deposited on a thin copper holder and then quenched in liquid propane. The frozen sample was fractured at −125°C in vacuo (about 10^{-7} Torr) with a liquid nitrogen-cooled knife in a Balzers 301 freeze-etching unit. The fractured sample was replicated with platinum-carbon (1–1.5 nm of metal deposit) backed with about 20 nm of carbon and the replica was cleaned with organic solvents, washed with distilled water and observed with a Philips 301 electron microscope. For each sample, two or three independent freezings, fractures and replicas were realized.

2.3. Freeze-etching electron microscopy

Alternative experiments were realized without glycerol as cryoprotectant. A small drop of dispersion was deposited on copper holders and frozen by rapid immersion in liquid nitrogen-cooled Freon 22. Fractures were performed on a Balzers BAF 300. Samples were fractured at −100°C and 10^{-6} Torr with a knife cooled at −196°C. The replicas were obtained by deposit under vacuum of a 2–4 nm platinum layer, then a 20–30 nm carbon layer. The replicas were immersed in a water-glycerol mixture (50% v/v), washed for 1 h at room temperature in sulfuric acid (80% v/v), rinsed three times with distilled water, and applied on copper grids (3 mm, 300 mesh).

2.4. Differential scanning calorimetry

For DSC measurements in the + 4–95°C temperature range, the F*n*C*m*PC samples were prepared by weighing the powdered phospholipid (2–3 mg) into the DSC pan and adding a weighed amount of deionized water (4–6 mg). Alternatively the phospholipids were dispersed by ultrasonication as described for the preparation of dispersions. 50–80 μl of dispersion were placed into the DSC pan which was immediately sealed and transferred to the calorimeters. For the DSC measurement performed on F6C4PC in the −20 to +35°C temperature range, 16 mg of F6C4PC and 3 mg of a water/ethylene glycol (70:30, w/w, to prevent freezing) were placed into the DSC pan. DSC measurements were carried out with Perkin Elmer DSC-2 and DSC-7 differential scanning calorimeters. Each sample was heated and cooled repeatedly at a rate of 2–5 C°/min and 10 C°/min, respectively. Transition enthalpies and temperatures were determined using the software provided. The reported values of the T_c represent the temperature at maximum excess heat capacity.

2.5. NMR spectroscopy

Samples for ^{31}P-NMR measurements were prepared by hydration of the phospholipids (5 mM) for 15 min, above their respective phase transition temperature, followed by several heating-cooling cycles with short vortexing times in the fluid phase. Samples were then transferred in 10 mm NMR tubes. ^{31}P-NMR spectra were obtained at 109.4 MHz on a Brucker WH 370 spectrometer. Typically 30000 scans were averaged in a quadrature mode detection. Spectra were acquired by

a fully phase cycled Hahn Echo sequence using the following parameters: 6.5 μs (90° flip angle) for the pulse, a 40 μs interpulse delay, a 13 μs (180° flip angle) for the second pulse and a 44 μs delay before acquisition. Spectra were obtained using a spectral width of 50 kHz, with broadband decoupling at maximal decoupling power during the pulses and acquisitions. Recycling times were of 6 and 10 s in the fluid and gel phases, respectively. The second spectral moments, $\mathcal{M}_2$, were calculated from the powder spectra using a Pascal program package [17]. The chemical shift anisotropies, $\Delta\sigma$, were determined directly from the spectra or calculated from $\mathcal{M}_2$ according to the relation $\mathcal{M}_2 = 16 \cdot \pi^2 \cdot \Delta\sigma^2/45$.

Samples for ^{19}F-NMR measurements (50 mM) were prepared by vortexing the phospholipids for 1 min above their T_c followed by short sonication (dial 5, pulse 50, 30 s) and by several heating-cooling cycles through their T_c. Proton decoupled ^{19}F spectra (0.1% CF_3COOH in D_2O as external reference, linewidth of

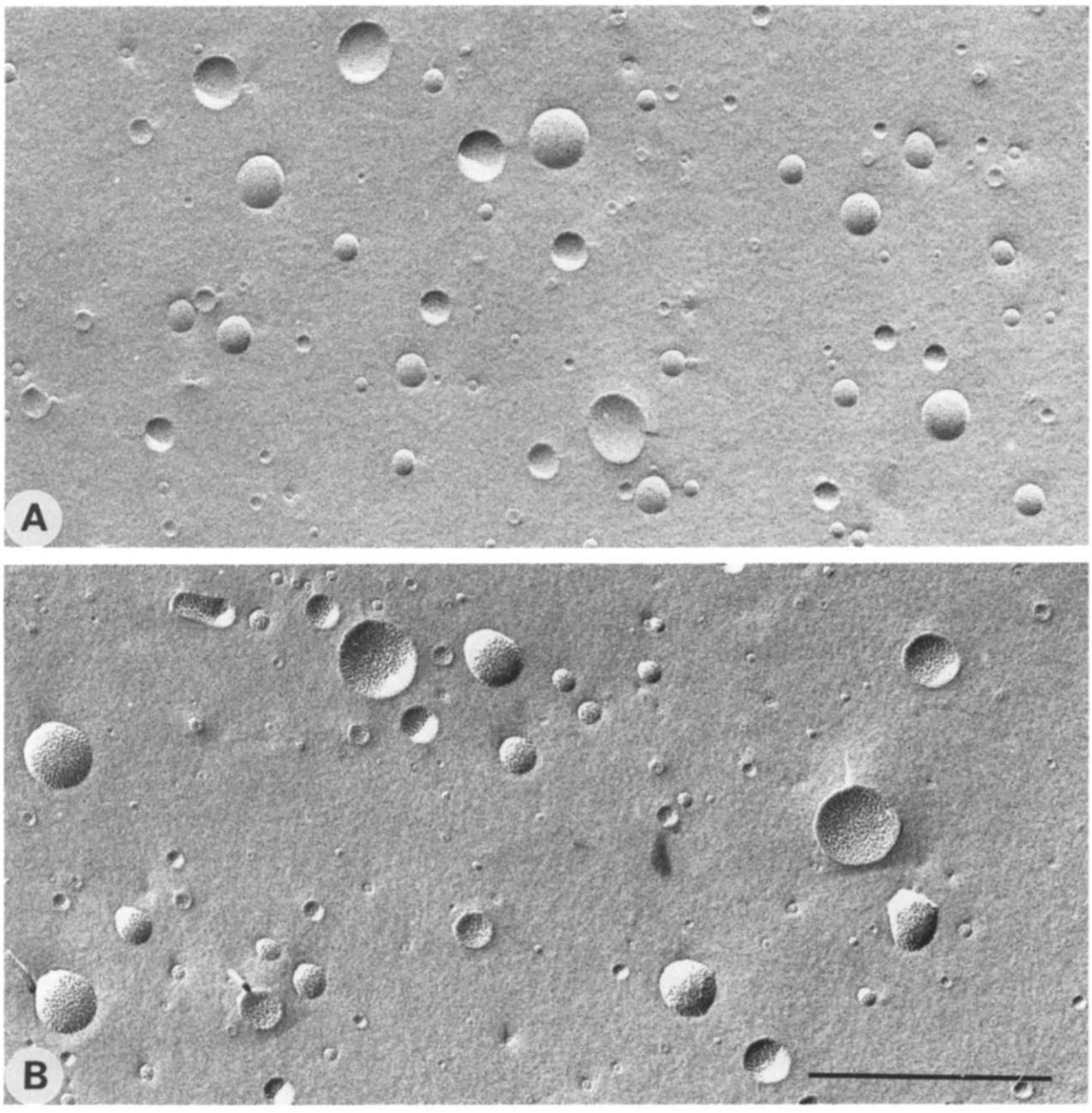

Fig. 2. Freeze-fracture electron micrographs of 3% w/v aqueous dispersions of F4C4PC and F6C4P prepared from thin layered or powdered lipids. (A) Dispersion of F4C4PC showing the presence of unilamellar vesicles. (B) Dispersion of F6C4PC showing the presence of mainly unilamellar vesicles displaying rougher fracture surfaces than F4C4PC. Scale bar is 500 nm.

1 Hz throughout the temperature range studied) were recorded on a Bruker AC 200 spectrometer at 188.3 MHz. Spectra were obtained using a spectral linewidth of 18 KHz using a 3 μs pulse (90° flip angle) and a recycling time of 1 s. The error in determining the linewidths is of approx. 10% (Hz). All spectra were recorded using broadband noise ^{1}H-decoupling at maximum decoupling power.

2.6. Electron paramagnetic resonance spectroscopy

A thin film of phospholipid was formed on the sides of a flask by evaporation to dryness under an argon stream of a $CHCl_3$/MeOH solution containing 35–40 μmol of the desired lipid. The film was further dried under vacuum (10^{-2} mmHg, 15 min). 200–300 μl of water were then added to the flask, which was shaken

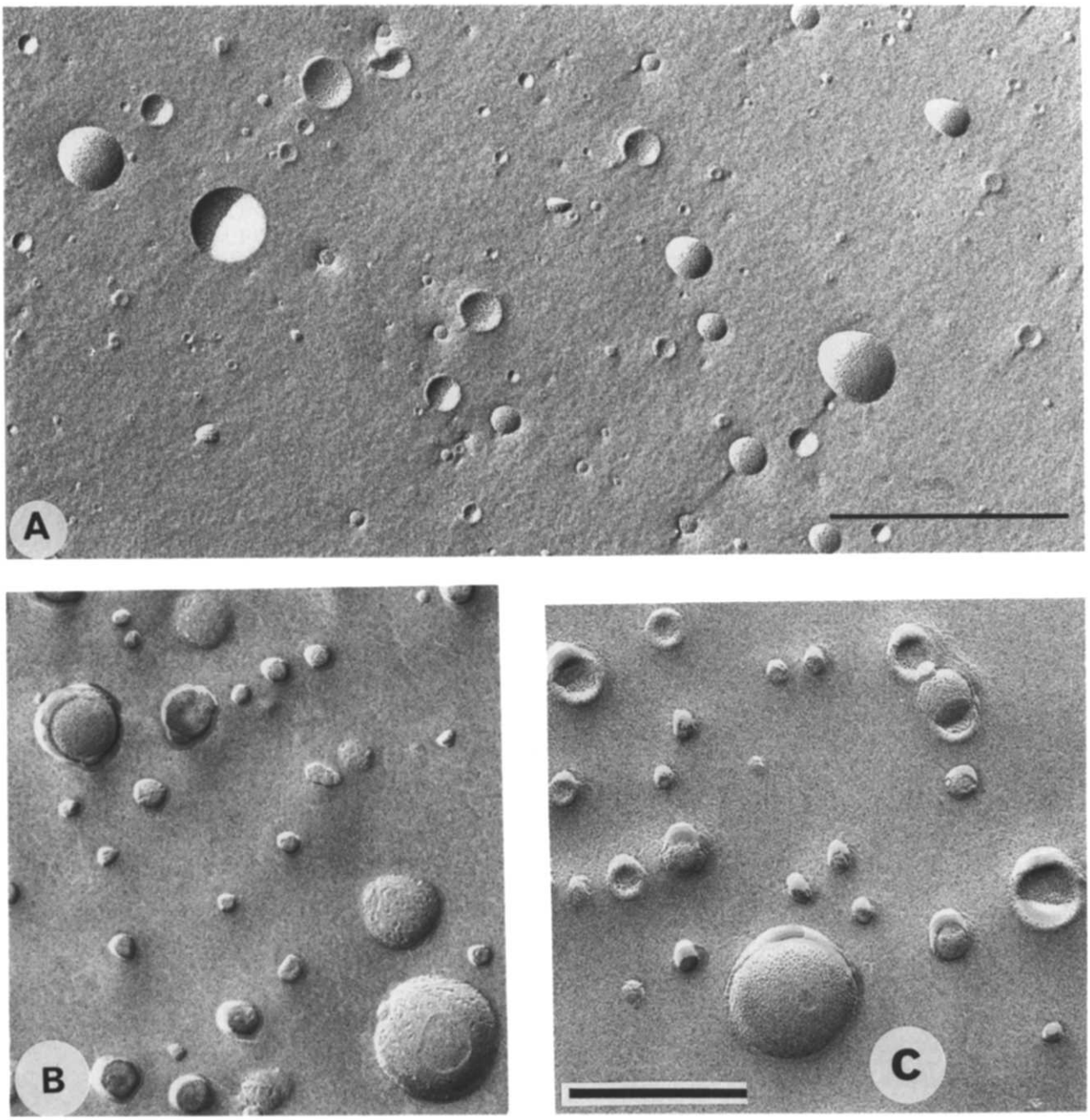

Fig. 3. Effect of heat sterilization on the morphology of vesicles prepared from F4C10PC. (A) Freeze-fracture electron micrograph of an unsterilized dispersion. (B) and (C) Freeze-etching electron micrographs of respectively unsterilized and sterilized dispersions. Note the similarity of these two preparations. Scale bars are 500 nm in (A) and 100 nm in (C). The scale bar in (C) stands also for (B).

vigorously on a vortex mixer for several minutes. Dispersions of compounds F6C10PC and F8C10PC were briefly sonicated (1 min, dial 4, pulse 50) in order to obtain stable dispersions. The temperature was kept above the phase transition temperature during agitation. A $5 \cdot 10^{-3}$ M aqueous solution of 2,2,6,6-tetramethylpiperidine-1-oxyl, Tempo, (30 μl) was added to the phospholipid dispersion which was then transferred to a capillary pipet used as a sample cell. The final lipid concentration was approx. 8–11% w/v. The spectra were recorded on a Brucker EPR 200 spectrometer.

3. Results

3.1. Freeze-fracture electron microscopy (FFEM), freeze-etching electron microscopy (FEEM) and light scattering spectroscopy (LSS) studies of the FnCmPC dispersions

Natural or synthetic phosphatidylcholines, when dispersed in excess of water and when energy is supplied, form uni- or multilamellar vesicles [18]. A similar behavior was observed in the case of the perfluoroalkylated amphiphiles F4C4PC, F6C4PC, F8C4PC and F4C10PC as shown by FFEM and FEEM of the replicas obtained according to well-established techniques [19]. For the preparation of the replicas, glycerol was added to prevent freeze damage. The replicas obtained without addition of glycerol gave similar results (not shown) with casual distortions or aggregation.

As illustrated in Figs. 2 and 3, samples of F4C4PC, F6C4PC, F8C4PC and F4C10PC, whether dispersed from the layered or from the powdered lipid using sonication, consist mainly in small and large spherical unilamellar vesicles and only of a few multilamellar ones (not shown). No difference in shape or size could be detected whatever the method of preparation. The same dispersions were also analyzed by LSS: the vesicles have average sizes of 100–140 nm, consistent with the particle sizes provided by electron microscopy.

On the other hand, both F6C10PC and F8C10PC, when dispersed at 80°C, show non-vesicular structures formed from stacked ribbon-like elements. These are particularly well seen on pellets resulting from the centrifugation of suspensions or with preparations obtained from hydrated powders. Examples of such structures are shown in Figs. 5 and 6 for compound F6C10PC. However, repeated heating/cooling cycles through the main phase transition temperature of F6C10PC, followed by sonication, allowed the preparation of stable dispersions consisting in unilamellar vesicles of 100 nm of average size (not shown).

Sterilized dispersions of F4C4PC, F6C4PC, F8C4PC, F4C10PC and F6C10PC (121°C, 15 min, 15 lb/in^2) were also examined by FFEM and/or by LSS. Freeze-fracture replicas of these sterilized dispersions show mainly unilamellar vesicles as illustrated in Fig. 3 for compound F4C10PC. Most importantly, Fig. 3 shows that the morphology of the vesicles prepared from F4C10PC was unaffected by the sterilization process. As evidenced by LSS measurements (Fig. 4), their average sizes, as well as those of sterilized dispersions of F4C4PC, F6C4PC, F8C4PC, F4C10PC and F6C10PC, were in the 100–140 nm range. For comparison, a 3% (w/v) DPPC dispersion prepared in the same conditions exhibited immediately after preparation two populations centered at 60 and 260 nm (Fig. 4); after sterilization a new, predominant population of large-sized vesicles (1150 nm) appeared.

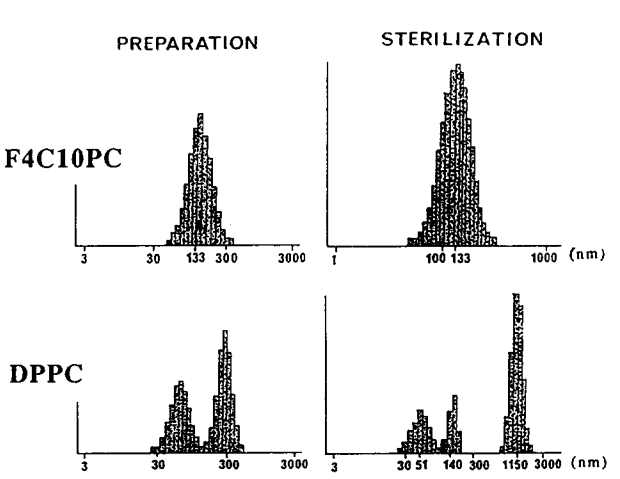

Fig. 4. Effect of heat sterilization on the particle size distribution of vesicles made from F4C10PC as compared to that of DPPC vesicles prepared under strictly the same conditions.

3.2. X-ray diffraction

In the presence of water and below T_c, the X-ray scattering spectra of F6C10PC preparations contain slightly diffuse small-angle reflections up to 12 Å^{-1}, and several sharp wide-angle reflections typical of rigid chains. The small angle spacing ratios are consistent with a rectangular-centered phase (see insert in Fig. 6) whose parameters are 140 and 82 Å (these parameters may vary according to the amount of water present within the phase). Above T_c, a lamellar L_α phase (105 Å) is observed with several sharp small-angle reflections and a diffuse band in the wide-angle scattering region. After cooling to room temperature, a lamellar gel phase is observed which persists for several days before the return to the initial rectangular-centered phase. The dimension of the lamellar phase can be as large as 145 Å, a value much larger than for hydrogenated phosphatidylcholines.

3.3. Differential scanning calorimetry

The thermotropic phase behavior of samples consisting of hydrated powders of the F*n*C*m*PCs was studied by DSC. Thus, when samples of F8C4PC, F4C10PC or F6C10PC are heated from 4°C up, a pretransition (except for F8C4PC) and a main phase transition are observed reproducibly (Table 1), even after the sample was taken repeatedly through several cooling-heating cycles.

The T_c and ΔH transition parameters of F6C10PC vary with the percentage of water present. Thus, increasing the water content from 66 to 88% w/w resulted, as expected, in a T_c and ΔH decrease from $T_c = 51$°C and $\Delta H = 0.6$ kcal/mol to $T_c = 43$°C and $\Delta H = 0.03$ kcal/mol for the pretransition, and from $T_c = 56.4$°C and $\Delta H = 7.0$ kcal/mol to $T_c = 48.0$°C and $\Delta H = 4.4$ kcal/mol for the main phase transition. For compound F8C4PC, the heating curve displays only a single transition at 69.3°C with an enthalpy of 2.4 kcal/mol (Table 1).

As evidenced by FFEM and/or ^{31}P-NMR (see below), F8C4PC, F4C10PC and F6C10PC, when dispersed in water, form a lamellar phase. It appears

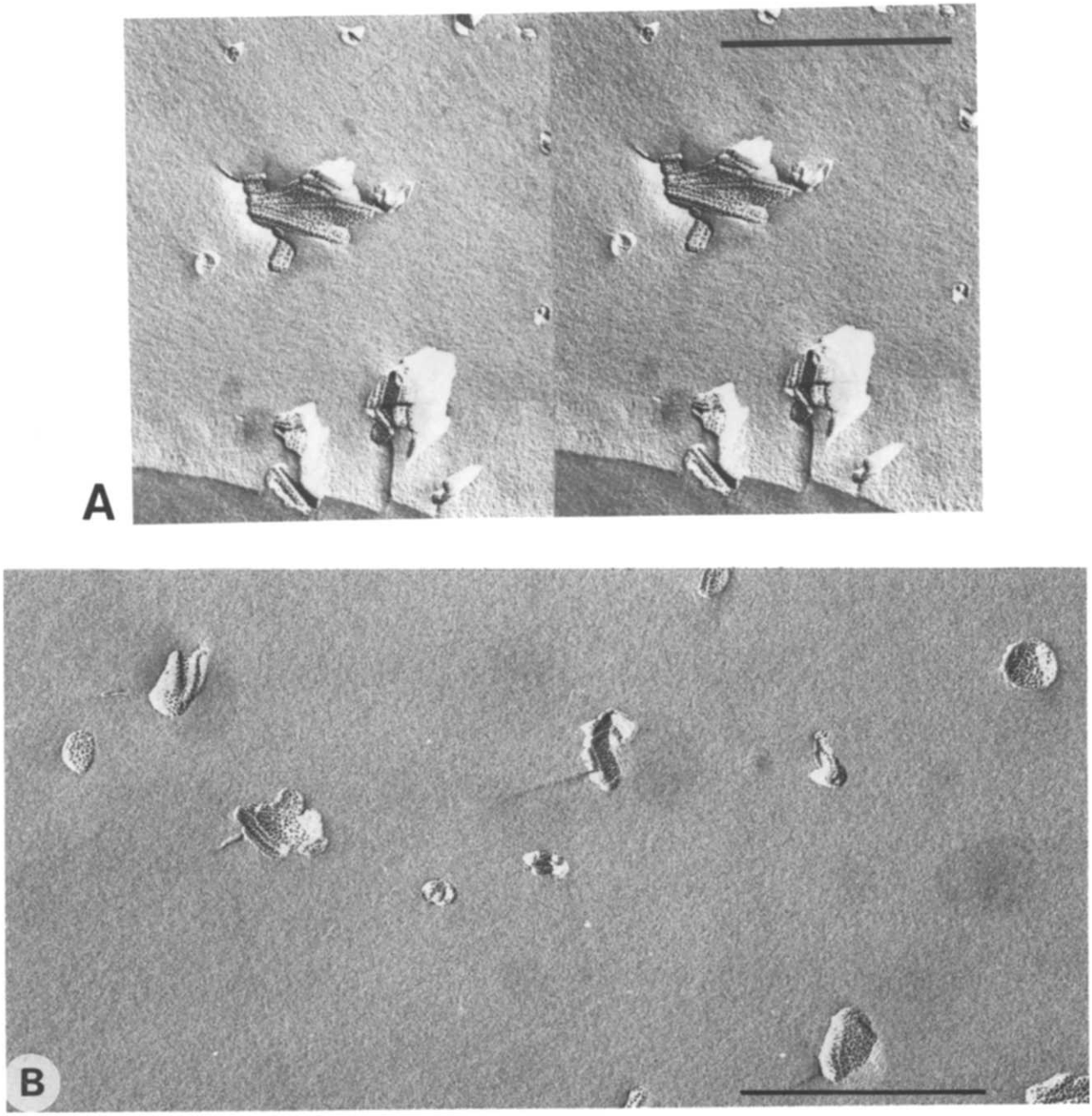

Fig. 5. Freeze-fracture electron micrograph of F6C10PC (3% w/v aqueous dispersion). (A) Stereo-pair images. (B) Enlarged view of the same dispersion. Scale bars are 500 nm.

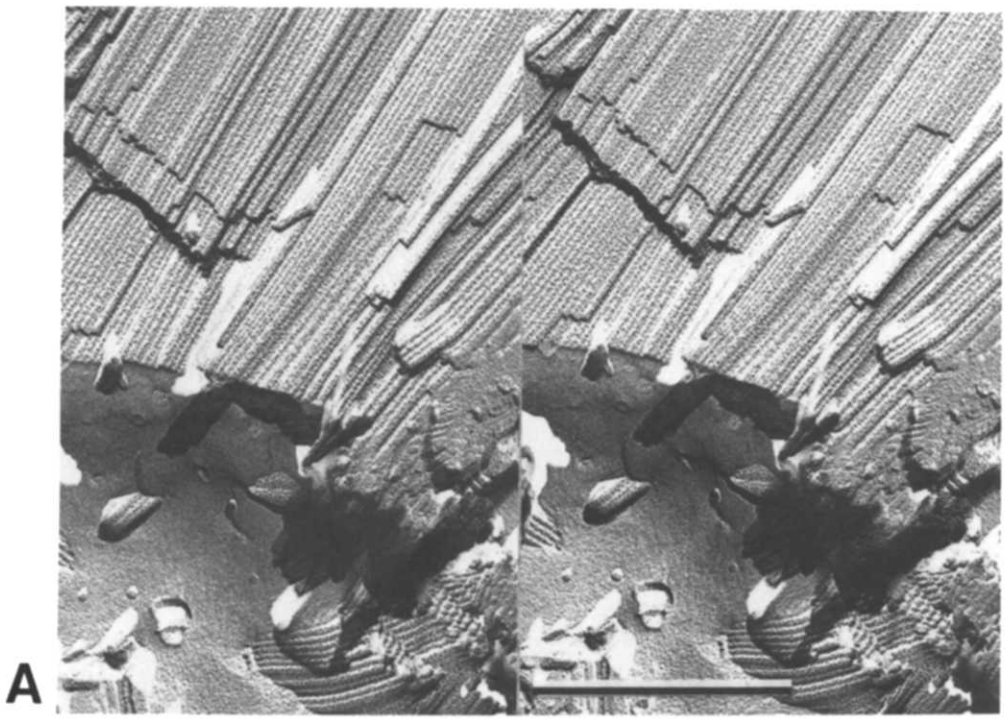

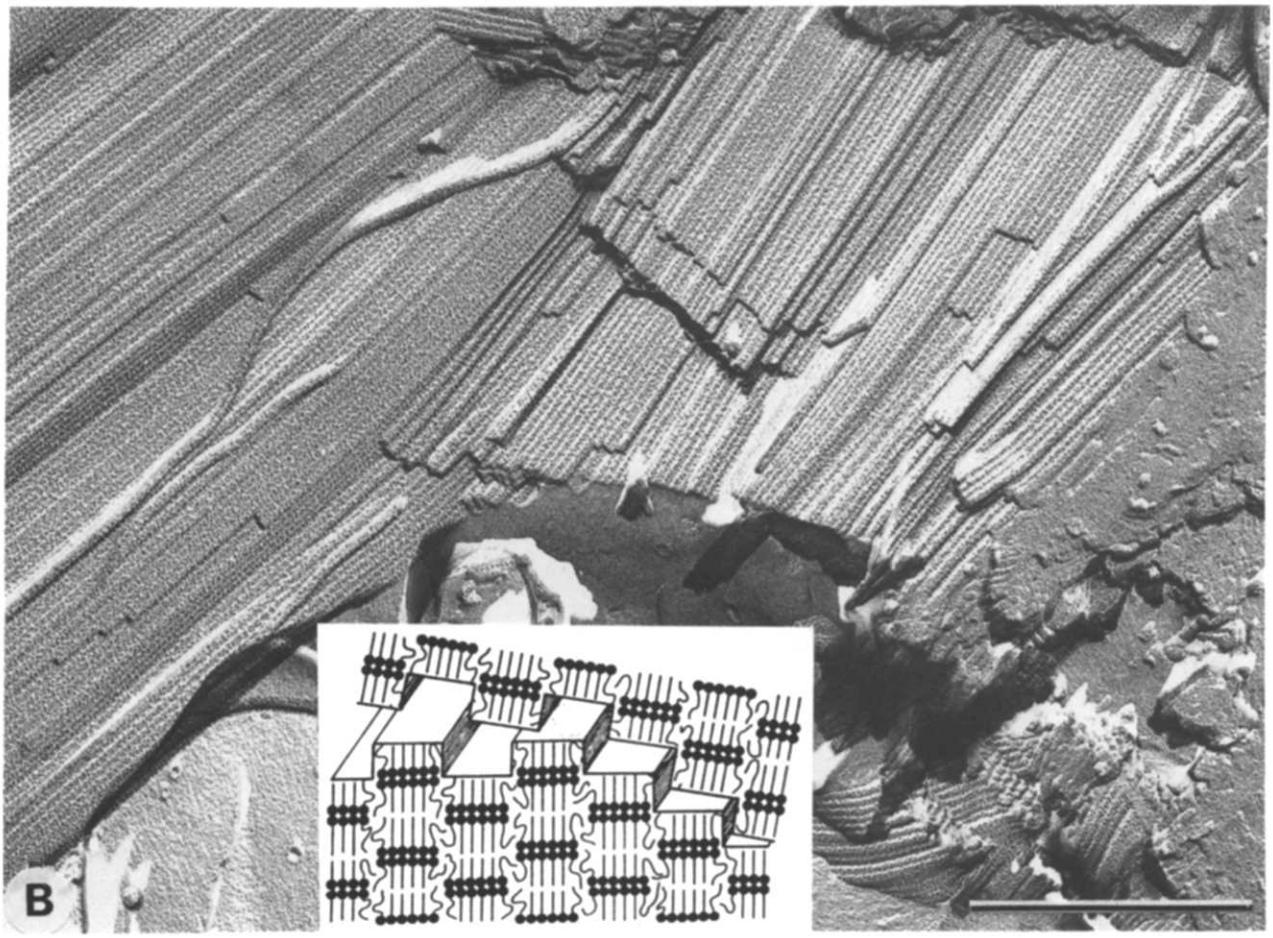

Fig. 6. Freeze-fracture images of a F6C10PC centrifugation pellet obtained from 3% w/v aqueous dispersion. (A) Stereo-pair images of the pellet. (B) Enlarged view of the same image. Note the roughness of the fractured surfaces and the presence of ribbon-like elements.

therefore, and by analogy with the hydrogenated phosphatidylcholines' phase behavior, that the pretransition and main phase transition observed by DSC for F4C10PC and F6C10PC can be assigned to a transition from a lamellar crystalline (gel) to a rippled gel phase and from a rippled gel to a lamellar liquid-crystalline (fluid) phase, respectively. In the case of F6C10PC, which forms also a ribbon-like phase, the pretransition could also be attributed to a ribbon-like to lamellar-gel phase transition. However, as evidenced by X-ray diffraction, this transition is only slowly reversible (several days). Furthermore, as shown by DSC, the pretransition is always measured at 42°C, even after several heating/cooling cycles. This most likely indicates that the pretransition is due to a lamellar-gel to rippled phase transition rather than to a ribbon-like to lamellar-gel phase transition.

The unique phase transition observed for F8C4PC is either a gel to fluid lamellar phase transition or, if the lamellar gel to rippled gel pretransition is energetically too low to be detected, a rippled gel to lamellar fluid transition.

By contrast, the heating curves of samples of F4C4PC and F6C4PC (66% of water content) showed no observable phase transition in the 4–95°C temperature range. Furthermore, no detectable phase transition was found in the −20 to +35°C temperature range for a concentrated sample of F6C4PC in a 70:30 w/w water/ethylene glycol solution (12% of water content). F4C4PC and F6C4PC form, indeed, a lamellar phase as evidenced by FFEM (vide supra). Thus, these DSC experiments most likely indicate that the gel to fluid phase transition occurs for these compounds at a temperature either lower than −20°C or in the −20–95°C range with an enthalpy too weak to allow its detection. However, when considering the effect of a decrease in chain length on T_c in the hydrogenated phosphatidylcholine series [18], it was found that a chain shortening of six methylenic carbon atoms is accompanied by a decrease in T_c of about 55°C (e.g., from T_c (DSPC) = 55°C to T_c (DLPC) = 0°C, see Fig. 10 and Table 1). On this basis F4C4PC and F6C4PC, which differ from F4C10PC and F6C10PC by six methylenic carbon atoms, respectively, are therefore expected to exhibit a gel to liquid-crystalline phase transition at a temperature lowered by 55°C than that of F4C10PC (T_c = 18.6°C) and F6C10PC (T_c = 48°C). This analysis, together with the DSC and ^{19}F-NMR data (see next section), most likely indicates that the main phase transition of F6C4PC (and a fortiori of F4C4PC which has shorter hydrophobic chains than F6C4PC) occurs at a temperature which can be reasonably estimated to be below 0°C.

No phase transition was observed for F8C10PC in the 4–95°C temperature range. Considering the effect of a chain length increase on ΔH and on T_c, F8C10PC is expected to exhibit a detectable gel to liquid-crystalline phase transition at a temperature higher than that of F8C4PC and a fortiori of F6C10PC. We conclude that the T_c of F8C10PC is likely to be higher than 95°C.

3.4. ^{19}F-NMR spectroscopy

Proton-decoupled ^{19}F-NMR spectra of compounds F4C4PC, F6C4PC, F8C4PC, and F4C10PC, dispersed

Table 1
Thermodynamic parameters of the phase transitions for the F*n*C*m*PCs and the hydrocarbon-PCs

Compound	% w/w water	Pretransition		Main transition		
		T_c (±1%°C)	ΔH (±5%) (kcal/mol)	T_c (±1%°C)	ΔH (±5%) (kcal/mol)	ΔS (cal/mol per K)
F*n*C*m*PC						
F4C4PC	66		[a]			
F6C4PC	66		[a]			
	16		[b]			
F8C4PC	66	[c]	[c]	69.3	2.4	7
F4C10PC	90	14	0.2	18.6	1.8	6.5
	90 [d]	low	low	15.9	1.9	
F6C10PC	66	51.0	0.6	56.4	7.0	
	88	43	0.03	48	4.4	13.7
F8C10PC	68		[a]			
Hydrocarbon-PC						
DLPC [e]	–	–	–	−1.8	1.7	5.6
DMPC [e]	–	–	–	23	5.4–6.7	18–22.5
DPPC [e]	–	–	–	41	8.7	28
DSPC [e]	–	–	–	55–58	10.7	32.5

[a] No transition detected between +4 and 95°C.
[b] No transition observed between −20 and +35°C.
[c] No pretransition observed.
[d] T_c and ΔH values measured upon cooling.
[e] T_c and ΔH values of the hydrocarbon-PCs are taken from Refs. 18a and 31.

in D_2O as vesicles, were recorded. An examination of the temperature dependence of the ^{19}F resonance's linewidth reveals dramatic changes induced by the gel to liquid-crystalline phase transition [20]. Fig. 7 shows the evolution of the linewidth vs. the temperature for the CF_3 and CF_2-CH_2 resonances for both F8C4PC (Fig. 7a) and F4C10PC (Fig. 7b) and for the resonance of the CF_2 α to the CF_3 group for F8C4PC (Fig. 7a). It can be seen that for both compounds the linewidths of the CF_3 and the methylene-bound CF_2 resonances decrease rapidly and level off at approximately 30°C and 50°C for F8C4PC, 13°C and 18°C for F4C10PC, respectively. The linewidth of the resonance of the CF_2 in α to the CF_3 group for F8C4PC levels off at approximately 30–35°C. These high resolution ^{19}F-NMR spectra indicate that rapid tumbling of the F*n* tails occurs for temperatures higher than 50°C and 18°C for F8C4PC and F4C10PC, respectively, which implies that the critical phase transition temperature is higher than

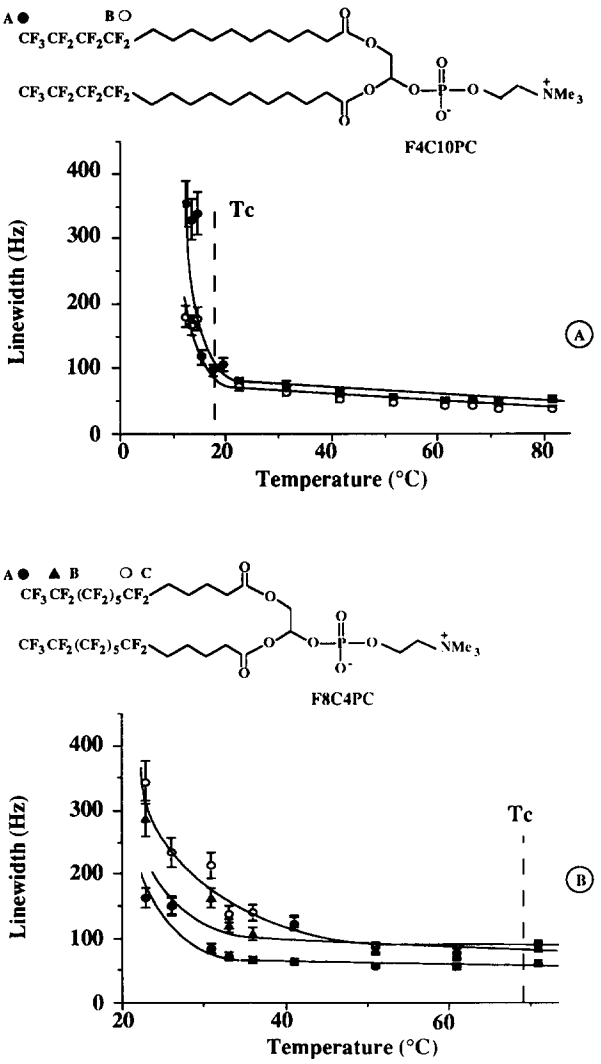

Fig. 7. Temperature dependence of the linewidths of the ^{19}F-NMR resonances of F4C10PC (A) and F8C4PC (B).

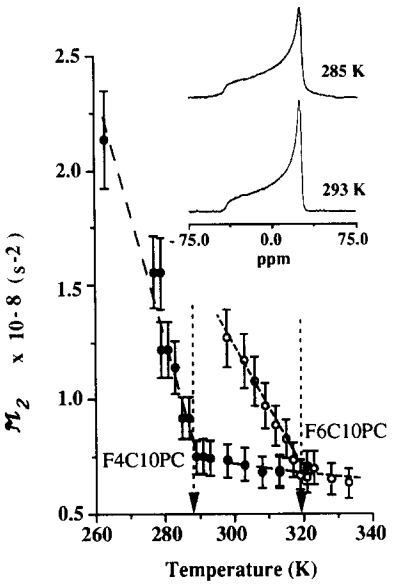

Fig. 8. Temperature dependence of the second spectral moment M_2 calculated from measured ^{31}P-NMR powder lineshapes (see inset) for dispersions of F4C10PC (●) and F6C10PC (○). Arrows indicate phase transition temperatures T_c.

or equal to 50°C for F8C4PC, and to 18°C for F4C10PC. These data are consistent with those obtained by DSC, i.e., 69.3°C for F8C4PC and 18.6°C for F4C10PC.

These ^{19}F-NMR experiments on F8C4PC and F4C10PC also show that, when rapid tumbling occurs, the linewidth of the CF_3 and CF_2-CH_2 resonances are in the 80–100 Hz range. For F4C4PC and F6C4PC, such linewidths are already found at about 14–18°C for both CF_3 and CF_2-CH_2 resonances, showing a rapid motion of the F*n* tail. We conclude that the T_c of both compounds is lower than or close to 18°C, in full agreement with the DSC data (see preceding section).

3.5. ^{31}P-NMR spectroscopy

Fig. 8 displays typical ^{31}P-NMR powder lineshapes measured between 278 and 335 K (see insert) for dispersions of F4C10PC and F6C10PC prepared by vortexing the phospholipid in D_2O and the temperature dependence of the second spectral moment M_2 calculated from these spectra [17]. Both compounds give rise to powder-type ^{31}P-NMR patterns consistent with a lamellar phase [21–23]. The axially symmetric lineshapes and chemical shift anisotropy tensor $\Delta\sigma$ of 42 ppm for F4C10PC at 291 K and of 39 ppm for F6C10PC at 328 K are, indeed, characteristic for phosphatidylcholines in a lamellar fluid state (see Table 2). The larger $\Delta\sigma$ values of 52 and 55 ppm measured for F4C10PC and F6C10PC, respectively, at 283 and 298 K (which reflect motional restriction of the phosphate head group) are characteristic for phosphatidylcholines in a lamellar gel state. The ^{31}P-NMR spectrum of

F6C10PC remained unchanged after storing the dispersion for more than 10 days at 298 K or even at 278 K.

Calculation of the second spectral moment, $\mathcal{M}_2$, provides a quantitative measurement of subtle changes that occur in the powder spectra which, in turn, are indicative of changes in motion of the phosphate group related to changes in the organization (gel to fluid phase transition for example) of the phospholipid [17]. As illustrated in Fig. 8, the second spectral moment $\mathcal{M}_2$ versus temperature curves display a break point at 288 and 319 K for F4C10PC and F6C10PC, respectively. This most likely arises from the gel to fluid phase transition of these lipids, in full agreement with the DSC data.

3.6. Electron paramagnetic resonance spectroscopy

EPR spectroscopy of the paramagnetic probe Tempo [24,25] dissolved in dispersions of the F*n*C*m*PCs was used to determine the phase transition temperature of the membranes they form and to evaluate the lipophilicity of these membranes. When the probe is added to an aqueous dispersion of membrane-forming amphiphiles, the resulting EPR spectrum consists in the superimposition of two spectra: one is due to Tempo dissolved in the hydrophobic core of the membrane, the other to the probe present in the aqueous phase (see Fig. 9). The amplitudes, h and p, of the two high-field hyperfine nitroxide signals are, in a first approximation, proportional to the amount of spin label dissolved in the membrane and in the aqueous region, respectively [24,25]. The change in the relative values of h and p as a function of temperature is a means of determining the phase transition temperature of the lipid. At this temperature an abrupt increase in solubility in the hydrophobic region, resulting in an increase of h, is expected. Fig. 9 illustrates the variations of the Tempo spectral parameter $f = h/p$ as a function of temperature for aqueous dispersions of different F*n*C*m*PCs and, for comparison, of DMPC and DPPC. It shows that only the behavior of F4C10PC parallels that of DMPC and DPPC, with an abrupt increase in f, when the temperature is raised over the gel to fluid phase transition temperature (as measured by DSC). Most importantly, Fig. 9 also shows that the solubility of Tempo in the hydrophobic region of the F*n*C*m*PCs F4C4PC, F6C4PC, F8C4PC, F6C10PC and F8C10PC is very low. Furthermore, no solubility enhancement was detected over the 0–95°C temperature range and a fortiori at the T_c of compounds F8C4PC and F6C10PC as determined by DSC. This demonstrates that the membranes formed by these *F*-alkylated amphiphiles are highly lipophobic, compared to those formed by F4C10PC, DMPC or DPPC.

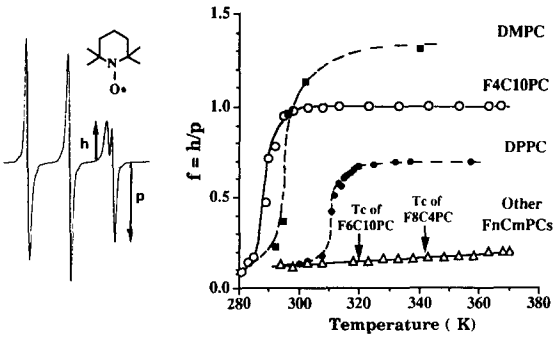

Fig. 9. Peak height ratio ($f = h/p$) as a function of temperature for Tempo partitioned between the hydrophilic and hydrophobic regions of F*n*C*m*PCs, DMPC and DPPC dispersions.

Table 2
^{31}P-NMR chemical shift anisotropy $\Delta\sigma$ (ppm) for F4C10PC and F6C10PC as compared to $\Delta\sigma$ values found for phosphatidylcholines (PC), phosphatidylethanolamines (PE) in the bilayer and hexagonal packing [21–23]

Phase		$\Delta\sigma$ PC (ppm)	$\Delta\sigma$ PE (ppm)	$\Delta\sigma$ F4C10PC (ppm)	$\Delta\sigma$ F6C10PC (ppm)
Bilayer	gel state	55–69	45–60	47–70 [a]	44–55 [c]
	fluid state	40–50	35–40	40–42 [b]	39–41 [d]
Hexagonal II		–	30–35	–	–

[a] From 14 to −10°C.
[b] From 40 to 16°C.
[c] From 45 to 25°C.
[d] From 60 to 47°C.

4. Discussion

Taken together, the data obtained from several different physical measurements demonstrate some unique properties of the new F*n*C*m*PCs. They illustrate the considerable effects caused by the introduction of perfluoroalkyl tails and the dependence of these effects on the lengths and relative weight of these tails in the total hydrophobic chain, hence by their fluorophilicity.

As evidenced by FFEM, the *F*-alkyl-PCs, F4C4PC, F6C4PC, F8C4PC and F4C10PC, like their hydrocarbon analogs, form liposomes, mainly unilamellar vesicles (see Fig. 2). This is also the case of F6C10PC but only after repeated heating/cooling cycles through its main phase transition temperature and sonication. However, F6C10PC and F8C10PC were found to exhibit an unusual, original phase behavior. Indeed, according to FFEM and X-ray diffraction, they display, as shown in Figs. 5 and 6, a 'ribbon-like' phase (two-dimensional centered rectangular lattice) when their dispersion is performed at 80°C followed by sonication at room temperature. To our knowledge, a ribbon-like phase such as that adopted by F6C10PC and F8C10PC has never been described. In the case of F6C10PC, this

phase converts, upon heating, into a lamellar phase. Upon cooling, the return to the ribbon-like phase is, however, very slow.

It is noticeable that the F*n*C*m*PCs form vesicles for a total hydrocarbon chain length (F*n* + C*m*) ranging from 8 to 16 atoms, whatever the length of the F*n* tail. In comparison hydrocarbon phosphatidylcholines form uni- or multilamellar vesicles for a lipidic chain length of 11–23 carbon atoms (lauryl to tetracosanoyl) and micelles when the chain length is shorter than 10 carbon atoms [18]. Replacing part of a hydrocarbon tail by a perfluoroalkyl one increases its hydrophobic character, hence enhances its amphiphilic character but reduces the inter- and intramolecular chain-chain interactions [26]. It appears that the associative forces which exist nevertheless between the lipidic chains (van der Waals attraction) and more importantly the hydrophobic interactions are sufficient in the case of the F*n*C*m*PCs to maintain a bilayer structure in water and even to generate such structures for chains as short as C_4F_9-$(CH_2)_4$-, as in F4C4PC. In this respect, it should be mentioned that even some single chain perfluoroalkylated phosphocholines are able to form stable vesicles and other supramolecular assemblies while their hydrogenated analogs do not [27].

We studied also the effect of the physical state of the lipid on the characteristics of F*n*C*m*PCs' dispersions. Our interest stemmed from the difference in behavior observed for dispersions prepared from thin layered or from powdered lipid in their ability to emulsify fluorocarbons [10]. Because these fluorinated lipids are destined for in vivo uses as liposome-forming amphiphiles or surfactants in injectable fluorocarbon emulsions, their dispersions require sterilization prior to use or storage. We therefore studied the effect of heat sterilization on the morphology of the dispersions of F*n*C*m*PCs.

Dispersions prepared either from thin-layered or from powdered F4C4PC, F6C4PC, F8C4PC and F4C10PC were analyzed before and after heat sterilization (standard norms) by FFEM and LSS (see Figs. 2,3, and 4). No structural modifications in the size or shape of the liposomes could be evidenced by these techniques which reveal a rather exceptional stability of these liposomes when submitted to such a drastic sterilization procedure. The average size measurements obtained by LSS remain, indeed, essentially unchanged. The resistance of the F*n*C*m*PCs' vesicles to sterilization contrasts strongly with that of DPPC dispersions for which a new and predominant population of large-sized vesicles appeared. The greater stability (in terms of particle sizes and particle size distribution) toward sterilization of the F*n*C*m*PC-based vesicles, as compared to that of DPPC liposomes, could arise from the increased hydrophobic character induced by the presence of the perfluoroalkyl tails [9,27].

In order to gain deeper insight into the original phase behavior of F6C10PC, which, as evidenced by FFEM and X-ray diffraction, displays a ribbon-like phase at room temperature and a lamellar phase above its phase transition temperature T_c, we further investigated this behavior by analysing the temperature dependence of its ^{31}P-NMR lineshape. ^{31}P-NMR spectroscopy provides a convenient diagnostic in the study of the polymorphic phase behavior of hydrated phospholipids [21–23]. This arises from the ability of the lipids to experience rapid axial rotation when in a bilayer organization, while in non-bilayer phases (hexagonal H_{II}, cubic...), additional motional averaging occurs due to lateral diffusion. These motions result in distinctive ^{31}P-NMR spectra for lipids involved in a bilayer phase, hexagonal H_{II} phase or phases such as inverted micellar or cubic packing. For example, phosphatidylcholines (PC) involved in a bilayer structure show an asymmetrical resonance with a highfield peak and a downfield shoulder, while phosphatidylethanolamines (PE) in the H_{II} phase exhibit lineshapes with a highfield shoulder. Furthermore, their spectra display distinctive characteristic $\Delta\sigma$ 'chemical shift anisotropy' (basal linewidth) values which are summarized in Table 2 for PC and PE.

We first assessed the validity of ^{31}P-NMR for the interpretation of the phase behavior of the F*n*C*m*PCs. As evidenced by FFEM, F4C10PC forms bilayer structures with a gel to fluid main phase transition occurring at 291 K according to DSC measurements. The insert in Fig. 9 displays typical ^{31}P-NMR spectra of F4C10PC recorded between 277 and 313 K: these spectral lineshapes indicate a bilayer morphology and the $\Delta\sigma$ values measured below and above T_c (Table 2) are concordant with the data for phosphatidylcholines in the gel and in the fluid lamellar phases, respectively [21–23]. Further, the second spectral moment $\mathcal{M}_2$ vs. temperature curve [17] (Fig. 9) shows the gel to fluid phase transition to occur at a temperature (288 K) very close to that measured by DSC (291 K).

We found that F6C10PC displays, in the whole temperature range investigated (from room temperature to 335 K), ^{31}P-NMR lineshapes and $\Delta\sigma$ values below and above its T_c (Table 2) which are very similar to those measured for F4C10PC. Furthermore, no modifications neither in lineshape nor in $\Delta\sigma$ were observed upon aging: the same spectra were indeed measured on a freshly prepared sample and after several days of storage at room temperature or even at 4°C. This may be interpreted to mean that F6C10PC forms a lamellar phase even at room temperature, but most likely indicates that ^{31}P-NMR does not allow to distinguish between a rectangular-centered ribbon-like phase and a lamellar phase. Nevertheless, the temperature dependency of the spectral moment $\mathcal{M}_2$ shows the main phase transition of F6C10PC to occur at 319 K

which is also very close to that measured by DSC (321 K in excess of water).

The thermotropic behavior of the F*n*C*m*PCs was investigated by DSC, ^{19}F- and ^{31}P-NMR and EPR. These techniques gave concordant data. The main phase transition parameters (enthalpy ΔH, critical gel to liquid-crystalline phase transition temperature T_c) could be directly measured by DSC for the lamellar-phase forming compounds F8C4PC, F4C10PC and F6C10PC only (Table 1). The ^{19}F resonance linewidth and/or DSC data analysis allowed us to estimate the T_c of the other two vesicle-forming derivatives F4C4PC and F6C4PC which are at least below 0°C, and the T_c of F8C10PC which is above 95°C (see Results section).

It is well known that the main phase transition of the lipid bilayer detected by DSC is an energetic event reflecting a cooperative transition of the bilayers from an ordered gel state to a disordered fluid state at T_c. The relative energetic contents and hence the relative packing modes of the lipid chains between two lipid bilayer systems can thus be compared on the basis of their thermodynamic parameters associated with the main phase transitions. The packing modes of the lipid chains can be conveniently described in terms of the conformational statistics (*trans*/*gauche* ratio), lateral chain-chain van der Waals and hydrophobic interactions. Consequently the observed changes in T_c, ΔH and ΔS values associated with the main phase transition may be attributed primarily to differences in the conformational statistics of the chains, lateral chain-chain and hydrophobic interactions of the respective *F*-alkyl-PCs and hydrocarbon-PCs in the gel state.

Thus, concerning the T_c, our results show, as illustrated in Fig. 10, that the T_c rises: (i) on increasing the F*n* tail's length for a given C*m* spacer (T_c of F8C4PC > T_c of F6C4PC, F4C4PC; T_c of F6C10PC > T_c of F4C10PC); (ii) on increasing the C*m* spacer's length for a given F*n* tail (T_c of F4C10PC > T_c of F4C4PC; T_c of F6C10PC > T_c of F6C4PC). A similar correlation between T_c, which is closely connected to the melting of the hydrophobic chains, and the alkyl-chain's length is observed for the hydrogenated phosphatidylcholines [18]. In the latter series, it was found that a monotonic chain lengthening of two methylenic carbon atoms is accompanied by a nearly monotonic T_c increase of about 20 °C (see Fig. 10a and Table 1). By contrast, a chain lengthening of two *F*-methylenic carbon atoms in the F*n*C*m*PC series, e.g., going from F6C4PC (T_c < 0°C) to F8C4PC (T_c = 69°C) or from F4C10PC (T_c = 18.6°C) to F6C10PC (T_c = 48°C), results in a larger T_c increase, e.g., an increase of at least 69 C° and 30 C°, respectively. A comparison between the T_c values of F8C4PC, F4C10PC and F6C10PC shows that the chain melting phase transition temperature is mainly modulated by the length of the F*n* segment rather than by the total chain length L (L = F*n* + C*m*). It was indeed expected that, when considering only L and by analogy with the hydrocarbon series, the phase transition of F8C4PC (L = 12) should be lower than that of F6C10PC (L = 16) and even lower than that of F4C10PC (L = 14). In fact, of the three compounds, it is F8C4PC, which has the shortest chain length but the longest perfluoroalkyl tail, which displays the highest T_c. It has been shown in other membrane-forming amphiphiles that introducing a C_8F_{17} fragment causes a significant increase of T_c [28] with respect to that of their hydrocarbon analogs. Accordingly we found also that the T_c of F8C4PC (69°C for L = 12) is higher than that of DMPC (23°C, L = 13), the nearest hydrocarbon analog (which possesses even one more carbon in its chains), and is even higher than that of DSPC (55°C) with its 17 carbon atom chains. Introducing a C_6F_{13} segment seems to have no effect on T_c: the T_c of F6C10PC (48°C, L = 16) is, as expected on the basis of L only, between those of DPPC (41°C, L = 15) and DSPC (55°C, L = 17). More surprising, the introduction of a short *F*-alkyl (C_4F_9) tail, as in F4C10PC, results in a decrease in T_c, as compared to DMPC, in spite of an increase of overall chain

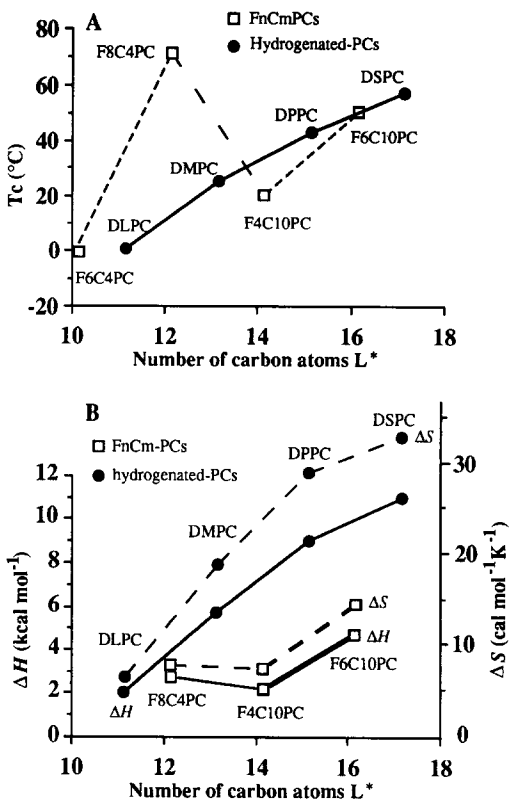

Fig. 10. (A) T_c and (B) ΔH and ΔS variations vs. length (number of carbon atoms, L) of the hydrophobic chain for the F*n*C*m*PCs and hydrocarbon-PCs. The T_c, ΔH and ΔS values of the hydrocarbon PCs were taken from Refs. 18a and 31. * For the F*n*C*m*PCs, $L = n + m$; for the hydrocarbon-PCs, L ($= p$) is the number of carbon atoms of the CH_3-$(CH_2)_{p-1}$-CO- chain (p = 11 for DLPC; p = 13 for DMPC; p = 15 for DPPC; p = 17 for DSPC).

length to 14 carbon atoms: the T_c of F4C10PC (18°C) is lower than that of DMPC (23°C) with 13 carbon atoms.

Concerning the ΔH and ΔS values measured for the main phase transition of F8C4PC, F4C10PC and F6C10PC, these values are much smaller, on the basis of the chain length, than those found for their corresponding hydrocarbon-PCs (Fig. 10b and Table 1). This indicates that the transition is mainly due to the reorganization of the hydrocarbon part of the F*n*C*m*PCs' chains and is further in line with studies performed on other fluorocarbon amphiphiles [28]. The ΔH and ΔS values in the hydrocarbon series are observed to increase nearly linearly with increasing chain length (Fig. 10b), reflecting that the packing interactions are perturbed proportionally to the chain length increase. In the F*n*C*m*PCs series, it appears that the perturbations are mainly governed by both the length and relative weight of the F*n* tail rather than by an overall chain length increase. The fact that we could not detect the phase transition for F4C4PC and F6C4PC makes it difficult to rationalize our results in terms of ΔH and ΔS increment per CF_2 and per CH_2 group for the F*n*C*m*PC series.

The apparent discrepancies observed between the F*n*C*m*PCs and hydrocarbon-PCs series concerning the T_c, ΔH and ΔS variations with the chain length are accounted for by recognizing that the introduction of a perfluoroalkylated chain can modulate the lipid packing order/disorder or the membrane's rigidity/fluidity in two opposite directions: (i) enhancement of packing disorder or fluidity, which results in a lowering in the thermodynamic parameters values, e.g., T_c, ΔH and ΔS, due mainly to weaker lateral inter- and intramolecular van der Waals interactions and increased steric repulsions between the fluorinated chains as compared with hydrocarbon chains [26], and (ii) increase in order or rigidity, which is only expressed here by an augmentation of T_c, related to an increase in hydrophobic interactions [29]. In the case of a short (C_4F_9) perfluoroalkyl tail the hydrophobic interactions are not likely to be sufficient to counterbalance the opposite effect. Thus, the replacement of part of the hydrocarbon chains by C_4F_9- appears to induce membrane fluidification. A C_6F_{13} tail is sufficient to equilibrate the antagonist contributions and does not modify the membrane fluidity. By contrast a C_8F_{17} segment results in the predominance of the hydrophobic interactions and enhances the membrane's rigidity.

The temperature dependence of the linewidth of the ^{19}F resonances was examined in order to circumvent the lack of sensitivity of DSC for the determination of the T_c. This further indicates, in the case of compound F8C4PC, that its phase transition is first induced by the melting of the F*n* tail and that each portion of the F*n* tail and the hydrocarbon spacer experience intrinsic changes of molecular motion with temperature [30]. Indeed, it is noticeable that, as shown in Fig. 7b, the melting of the C_8F_{17} chain of F8C4PC starts at approx. 30°C with the terminal CF_3 group, continues at 35°C with the CF_2 in α of the CF_3 group, and finishes with the CF_2 close to the C*m* spacer at nearly 50°C, a temperature which is still far below the T_c of the main phase transition (69°C). That the melting of the perfluoroalkyl chains occurs over such a large temperature range (almost 20°C) is in marked contrast with the hydrogenated phosphatidylcholines' behavior for which chain melting, due to high cooperativity, occurs within a very short temperature range (1°C) at their phase transition temperature [18b]. In F4C10PC, both the terminal CF_3 and $CF_2(\text{-}CH_2)$ groups of the shorter C_4F_9 tail start moving within a temperature range of only 2–4°C and at a temperature close to the T_c (Fig. 7a). The gel to liquid-crystalline transition of the chains in compound F4C10PC appears to exhibit greater cooperativity than in F8C4PC. While replacing a short hydrocarbon portion by the corresponding *F*-alkyl segment maintains the cooperative effects which characterize the phase transition of hydrocarbon phosphatidylcholines, longer *F*-alkyl chains behave as if the different fragments along the chain's skeleton entered molecular motion 'individually'.

The partitioning of the lipophilic/hydrophilic paramagnetic probe Tempo between the aqueous and lipidic phases present in the F*n*C*m*PC dispersions was investigated by temperature dependence EPR experiments throughout a larger temperature range and particularly beyond the gel to fluid phase transitions of these F*n*C*m*PCs. These experiments were intended to evaluate the impact of the *F*-alkyl tails on the lipophilicity of the phospholipid vesicle's shell, hence on the solubility of lipidic compounds into the core of such membranes. We found, as illustrated in Fig. 9, that an increase in fluorophilicity results in a dramatic decrease of the membrane's lipophilicity. Thus, F4C10PC, the least fluorophilic (shortest F*n* tail) but also the most lipophilic (lowest F*n*/C*m* ratio) of the *F*-alkyl-PCs investigated, exhibits a Tempo distribution comparable to that of DMPC; this partitioning is, as expected, strongly enhanced at the compound's gel to fluid phase transition temperature (18.0°C). By contrast, the spin probe was found to be located only in the aqueous phase in the presence of vesicles based on the other *F*-alkyl-PCs, which have longer fluorinated chains or higher F*n*/C*m* ratio. This is in particular the case of vesicles based on F4C4PC or F6C4PC whose main phase transitions occur at temperatures lower than of F4C10PC. Such a low solubility of the lipophilic probe in the fluorophilic/lipophilic core of the vesicles most likely arises from an increase of the membrane's fluorophilic character at the expense of its lipophilic character. To a lesser extent, it could also arise from an increased order of the fluorinated membranes in

their fluid state. As a consequence, the high stability of the vesicles and the low lipophilicity and increased order of the membranes formed by the new *F*-alkyl-PCs will undoubtedly modify their interactions with, more particularly, hydrophobic proteins, peptides, enzymes, cells and may have therefore interesting potential in drug delivery systems.

5. Acknowledgements

We would like to extend our grateful thanks to Drs. Eric J. Dufourc and Bernard Septe for their help in performing the NMR analysis and for helpful discussions. We thank the CNRS and ATTA for financial support.

6. References

[1] (a) Fendler, J.H. (1982) Membrane Mimetic Chemistry, Wiley, New York.
(b) Bangham, A.D. (1980) in Liposomes in Biological Systems (Gregoriadis, G. and Allison, A.C, eds.), Wiley, New York.
[2] Gregoriadis, G. (1988) Liposomes as Drug Carriers: Recent Trends and Progress, Wiley, Chichester.
[3] (a) Long, D.C., Long, D.M., Riess, J.G., Follana, R., Burgan, A. and Mattrey, R.F. (1989) in Blood Substitutes (Chang T.M.S. and Geyer R.P, eds.), pp. 441–442, Marcel Dekker, New York.
(b) Riess, J.G., Dalfors, J.L., Hanna, G.K., Klein, D.H., Krafft, M.-P., Pelura, T.J. and Schutt, E.G. (1992) Biomater. Artif. Cells Immob. Biotech. 20, 839–842.
[4] Riess, J.G. (1988) Curr. Surg. 45, 365–370.
[5] Riess J.G. (1993) in Blood Substitutes and Oxygen Carriers (Chang, T.M.S., ed.), pp. 24–43, M. Dekker, New York.
[6] Riess, J.G. (1991) in Blood Compatible Materials and Devices, Prospectives towards the 21st Century, pp. 237–270, Technomics, Lancaster, PA.
[7] (a) Riess, J.G. (1991) Int. J. Artif. Org. 14, 225–258.
(b) Riess, J.G. (1991) Artif. Org. 15, 408–413.
[8] (a) Santaella, C., Vierling, P. and Riess, J.G. (1991) New J. Chem. 15, 685–692.
(b) Greiner, J., Riess, J.G. and Vierling, P. (1993) in Organofluorine Compounds in Medicinal Chemistry and Biomedical Applications (Filler, R., Kobayashi, Y. and Yagupolskii, L.M., eds.), pp. 339–380, Elsevier, Amsterdam.
[9] Santaella, C., Vierling, P. and Riess, J.G. (1991) Angew. Chem. Int. Edn. Engl. 30, 567–568.
[10] (a) Santaella, C., Vierling, P. and Riess, J.G. (1992) New J. Chem. 16, 399–404.
(b) Santaella, C.; Vierling, P. and Riess, J.G. (1991) J. Colloid. Interf. Sci. 148, 288–290.
[11] Israelachvili, J.N. (1985) Intermolecular and Surface Forces, Academic Press, London.
[12] Cevc, G. and Marsh, D. (1987) in Phospholipid Bilayers, Wiley Interscience, New York; Cevc, G. (1991) Biochemistry 30, 7186–7193.
[13] Oldfield, E., Lee, R.W.K., Meadows, M., Dowd, S.R. and Ho, C. (1980) J. Biol. Chem. 24, 11652.
[14] (a) Longmuir, K.J., Capaldi, R.A. and Dahiquist, F.W. (1977) Biochemistry 16, 5746–5755.
(b) Gent, M.P.N., Armitage, I.M. and Prestegard, J.H. (1976) J. Am. Chem. Soc. 98, 3749–3755.
[15] Sturtevant, J.M., Ho, C. and Reimann, A. (1979) Proc. Natl. Acad. Sci. USA 76, 2239–2243.
[16] Cavanaugh, J.R., Pfeffer, P.E. and Valentine, K. (1986) Chem. Phys Lipids 39, 193–202.
[17] (a) Dufourc, E.J., Mayer, C., Stohrer, J. and Kothe, G. (1992) J. Chim. Phys. 89, 243–252.
(b) Dufourc, E.J., Mayer, C., Stohrer, J., Althoff, G. and Kothe, G. (1992) Biophys. J. 61, 42–57.
[18] (a) New, R.R.C. (1990) Liposomes, a Practical Approach, Oxford University Press, New York.
(b) Puisieux, F. and Delattre, J. (1985) Les Liposomes, Applications Thérapeutiques, pp. 1–34, Technique et Documentation Lavoisier, Paris.
(c) Chapman, D. (1983) in Liposome Technology: Preparation of Liposomes (Gregoriadis G., ed.), Vol. 1, pp. 11–13, CRC Press, Boca Raton, FL.
[19] Gulik-Krzywicki, T., Aggerbeck, L.P. and Larsson, K. (1984) in Surfactants in Solution (Mittal, K.L. and Lindman, B., eds.), Vol. 1, pp. 237–257, Plenum Press.
[20] Gent, M.P.N. and Ho, C. (1978) Biochemistry 17, 3023–3038.
[21] Seelig, J. (1978) Biochim. Biophys. Acta 515, 105–140.
[22] Griffin, R.G. (1976) J. Am. Chem. Soc. 98, 851–853.
[23] (a) Tilcock, C.P.S., Cullis, P.R. and Gruner, S.M. (1986) Chem. Phys. Lipids 40, 47–56.
(b) Cullis, P.R. and De Kruijff, B. (1978) Biochim. Biophys. Acta 507, 207–218.
(c) Cullis, P.R. and McLaughin, A.C. (1977) Trends Biochem. Sci. 2, 196–199.
(d) Cullis, P.R. and De Kruijff, B. (1976) Biochim. Biophys. Acta 436, 523–540.
(e) McLaughin, A.C., Cullis, P.R., Berden, J.A. and Richards, R.E. (1975) J. Magn. Reson. 20, 146–165.
[24] Shimshick, E.J. and McConnel, H.M. (1973) Biochemistry 12, 2351–2360.
[25] Kusumi, A., Singh, M., Tirell, D.A., Oehe, G., Singh, A., Samuel, N.P.K., Hyde, J.S. and Regen, S. (1983) J. Am. Chem. Soc. 105, 2975–2980.
[26] Mukerjee, P. (1981) J. Phys. Chem. 85, 2298–2303.
[27] Krafft, M.-P., Guilieri, F. and Riess, J.G. (1993) Angew. Chem. Int. Edn. Engl. 32, 741–743.
[28] Kunitake, T., Ando, R. and Ishikawa, Y. (1986) Mem. Fac. Kyushu Univ. 46, 231–243.
[29] Hargreaves, W.R. and Deamer, D.W. (1978) Biochemistry 18, 3759–3768.
[30] Higashi, N., Matsumoto, T. and Niwa, M. (1988) Science and Engineering Review of Doshisha University 29, 24–28.
[31] Mabrey, S. and Sturtevant, J.M. (1976) Proc. Natl. Acad. Sci. USA 73, 3862–3866.